Design of a Planar Ultrawideband Antenna With a New Band-Notch Structure

Chong-Yu Hong, Ching-Wei Ling, I-Young Tarn, and Shyh-Jong Chung, *Senior Member, IEEE*

***Abstract*—A novel planar ultrawideband (UWB) antenna with band-notched function. The antenna consists of a radiation patch that has an arc-shaped edge and a partially modified ground plane. The antenna that makes it different from the traditional monopole antenna is the modification in the shape of ground plane, including two bevel slots on the upper edge and two semicircle slots on the bottom edge of the ground plane. These slots improve the input impedance bandwidth and the high frequency radiation performance. With this design, the return loss is lower than 10 dB in 3.1–10.6 GHz frequency range and the radiation pattern is highly similar to the monopole antenna. By embedding a pair of T-shaped stubs inside an elliptical slot cut in the radiation patch, a notch around 5.5 GHz WLAN band is obtained. The average gain is lower than − 18 dBi in the stopband, while the patterns and the gains at frequencies other than in the stopband are similar to that of the antenna without the band-notched function.**

***Index Terms*—Band-notched antennas, planar antennas, ultra wideband (UWB).**

I. Introduction

THE FEDERAL Communication Commission (FCC)'s allocation of the frequency band 3.1–10.6 GHz [1] for commercial use has a sparked attention on ultrawideband (UWB) antenna technology in the industry and academia. The UWB systems can be divided into two categories: direct sequence UWB (DS-UWB) and multiband orthogonal frequency division multiplexing (MB-OFDM). The DS-UWB proposal foresees two different carrier frequencies at 4.104 (low band) and 8.208 GHz (high band). By the MB-OFDM format in 802.15.3a, the interval between 3.1 and 10.6 GHz is divided into 13 sub-intervals. Each sub-interval corresponds to one band of the MB-OFDM, with the bandwidth of 528 MHz [2], [3].

The UWB antennas proposed in the open literature mainly focus on the slot and monopole antenna. Printed wide slot antennas have an attractive property of providing a wide operating bandwidth, especially for those having a modified tuning stub, such as the fork-like stub [4]–[7], the rectangular stub [8], [9], and the circular stub [10] inside the wide slot. Broadband planar monopole antennas have received considerable attention owing to their attractive merits, such as ultrawide frequency band, good radiation properties, simple structure and the ease of fabrication. The typical shapes of these antennas are half-disc [11], circle, ellipse [12], [13], and rectangle [14].

Despite the approval of the FCC for UWB to operate over 3.1 to 10.6 GHz, it may be necessary to notch-out portions of the band in order to avoid interference with the existing wireless networking technologies such as IEEE 802.11a in the U.S. (5.15–5.35 GHz, 5.725–5.825 GHz) and HIPERLAN/2 in Europe (5.15–5.35 GHz, 5.47–5.725 GHz). This is due to the fact that UWB transmitters should not cause any electromagnetic interference to nearby communication system such as the wireless local area network (WLAN) applications. Therefore, UWB antennas with notched characteristics in the WLAN frequency band are required. There are various methods to achieve the band-notched function. The conventional methods are cutting a slot (i.e., U-shaped, arc-shaped, and a pie-shaped slot) on the patch [15]–[19], inserting a slit on the patch [20]–[22], or embedding a quarter-wavelength tuning stub within a large slot on the patch [23]. Another way is putting parasitic elements near the printed monopole as filters to reject the limited band [24] or introducing a parasitic open-circuit element, rather than modifying the structure of the antenna's tuning stub [25].

In this paper, a microstrip-fed planar UWB antenna is proposed. The arc-shaped edge radiation patch and the two bevels on the upper edge of the ground plane cause a wide bandwidth from 3 to 10 GHz for UWB application. Additionally, two semicircle slots cut on the bottom edge of the ground plane further improve the high frequency performances, including the impedance matching and radiation characteristics. The notched band, covering the 5-GHz WiFi band, is achieved by an equivalent parallel LC circuit formed by two T-shaped stubs inside an ellipse slot cut in the radiation patch. This approach provides more degrees of freedom in design, and is capable of producing a steeper rise in VSWR curve at the notch frequency. The antenna has a compact size of 24 mm $\times$ 35 mm $\times$ 0.8 mm. The measured 10-dB return loss shows that the proposed antenna achieves a bandwidth ranging from 2.95 to over 11 GHz with a notched band of 5–6 GHz. The proposed antenna presents omnidirectional patterns across the whole operating band in the H-plane.

Section II presents the geometry of the proposed UWB antenna. The effects on the impedance bandwidth are then analyzed, including full band and band-notched function designs. After that, the measured return losses and radiation patterns are presented in Section IV. Section V gives the conclusions.

II. Antenna Configuration

Fig. 1 shows the geometry of the proposed antenna. It consists of a radiation patch with an arc-shaped edge and a partially

Manuscript received May 11, 2007; revised July 30, 2007. This work was supported in part by the National Science Council, R.O.C., under Contract NSC 96-2752-E-009-003-PAE.

C.-Y. Hong was with Department of Communication Engineering, National Chiao Tung University, Hsinchu, Taiwan 30050, R.O.C. He is now with the Chi Mei Communication Systems Incorporation, Taipei, Taiwan, R.O.C.

C.-W. Ling, I.-Y. Tarn, and S.-J. Chung are with the Department of Communication Engineering, National Chiao Tung University, Hsinchu, Taiwan 30050, R.O.C. (e-mail: sjchung@cm.nctu.edu.tw).

Digital Object Identifier 10.1109/TAP.2007.910486

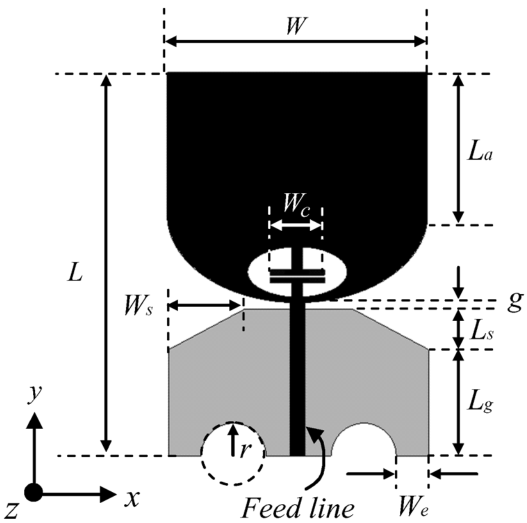

Fig. 1. Geometry of the proposed antenna. $W \times L = 24$ mm × 35 mm, $L_a = 13$ mm, $g = 0.6$ mm, $L_g = 9.7, W_s \times L_s = 7$ mm × 3.7 mm, $W_c = 3.6$ mm, $W_e = 3$ mm, $r = 3$ mm.

modified ground plane with two bevels to achieve a broad bandwidth. The arc-shaped edge of the radiation patch is a half-ellipse with the major axis of 8 mm and the axial ratio of 1.5. The lengths and width of the straight-edges of the radiation patch are L_a and W, respectively. The bevels with dimensions of $W_s \times L_s$ are placed on the upper side of the ground plane. Additionally, the antenna performance in the high frequency band can be further improved by cutting two semicircle slots on the bottom side of the ground plane. The two semicircle slots have the same radii of r and are placed W_e away from the side edge of the ground plane. The gap between radiation patch and ground plane is denoted as g. A 50 Ω microstrip line of 1.5 mm width is connected to the radiation patch as the feed line. Moreover, an elliptical slot cut in the radiation patch with a pair of T-shaped stubs embedded inside produces a notched band in the vicinity of 5.5 GHz and thus prevents the interference with the WLAN system. The antenna is printed on both the top (the radiation patch and microstrip line) and back-side (the ground plane) of a FR4 substrate with thickness of 0.8 mm, relative permittivity of 4.4, and loss tangent of 0.02. The total antenna size is 24 mm × 35 mm.

III. Antenna Design

In this section, the antenna covering the full UWB band (3.1–10.6 GHz) is first described. Then, the new band-notched structure, which is equivalent to a parallel LC circuit, is investigated. The effects with respect to the geometric parameters of the proposed antenna on impedance bandwidth and radiation pattern are discussed. The proposed antenna structure is simulated using the Ansoft High Frequency Structure Simulator (HFSS) [26], which is a commercial 3-D full-wave electromagnetic simulation software.

A. Full Band UWB Antenna Design

At low frequencies, the current is mainly distributed over the radiation patch and the ground plane, which is similar to the current of a printed finite-ground monopole antenna. Thus, increasing the patch length L_a is equal to increasing equivalent current length and decreasing the resonant frequency. Fig. 2 shows the simulated return losses for L_a varied from 7 to 13 mm. It can be seen that the edge of low frequency decrease as L_a increase. When L_a varies from 7 to 13 mm, the low frequency edge moves from 3.25 to 2.75 GHz.

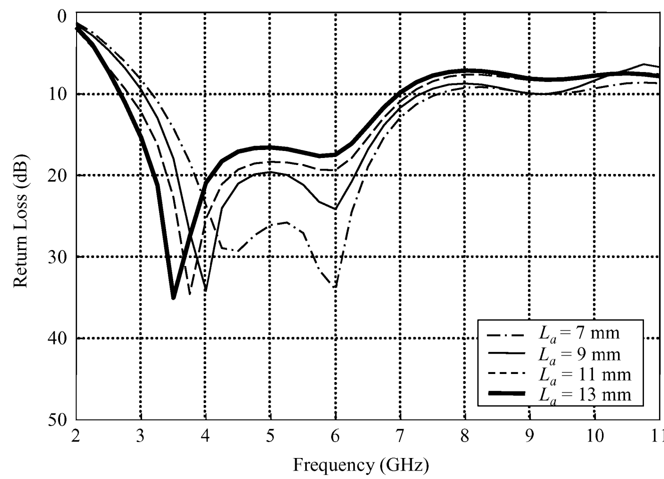

Fig. 2. Simulated return losses for the proposed antenna with various patch length L_a. $W_s = L_s = W_c = W_e = r = 0$ mm. Other geometric parameters are the same as given in Fig. 1.

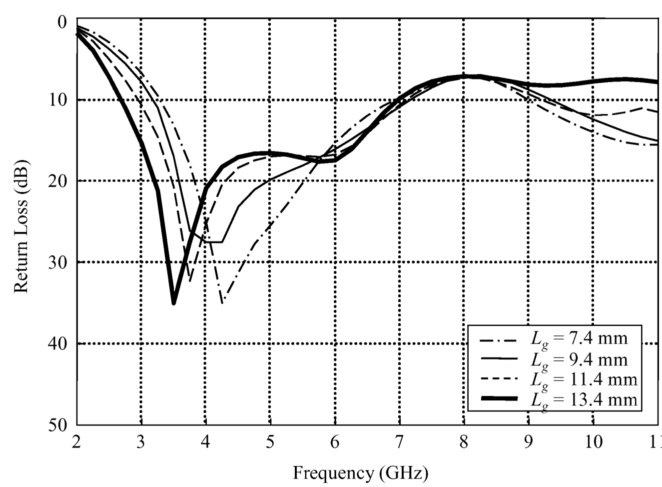

Fig. 3. Simulated return losses for the proposed antenna with various ground plane length L_g. Other geometric parameters are the same as given in Fig. 2.

The ground plane of the proposed antenna is also a part of the antenna. The current distribution on the ground plane affects the characteristics of the antenna. The monopole antenna as well as the ground plane forms an equivalent dipole antenna. Fig. 3 shows the effects of varying the ground plane length L_g ($L_g =$ 7.4, 9.4, 11.4, and 13.4 mm) on the simulated return losses, with $L_a = 13$ mm. In Fig. 3, the edge of low frequency decreases as L_g increases, the behavior is similar to changing L_a. When L_g varies from 7.4 to 13.4 mm, the edge of low frequency moves from 3.5 to 2.75 GHz.

The gap between the radiation patch and the ground plane has an important effect on the impedance matching of the proposed antenna, as shown in Fig. 4. When the gap g is increasing from

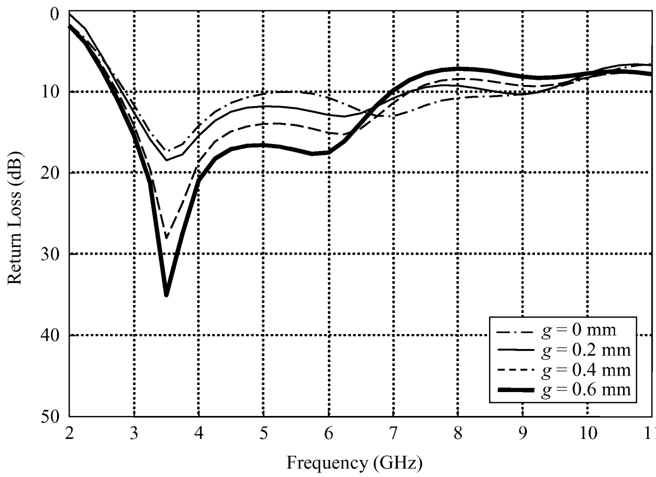

Fig. 4. Simulated return losses for the proposed antenna with various gap g. Other geometric parameters are the same as given in Fig. 2.

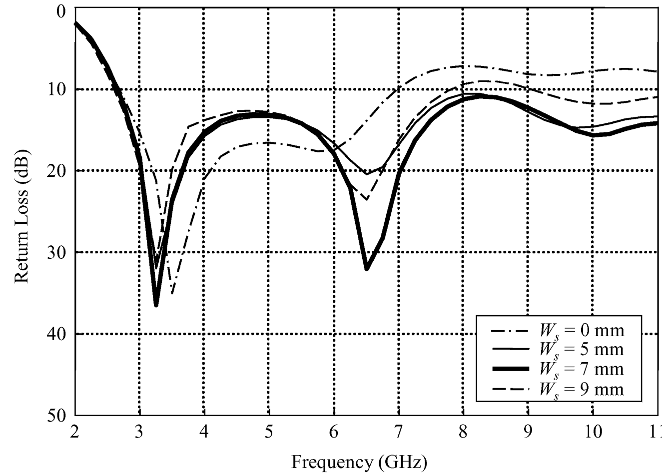

Fig. 6. Simulated return losses for the proposed antenna of various bevel width W_s with a fixed value of $L_s = 3.7$ mm. Other geometric parameters are the same as given in Fig. 2.

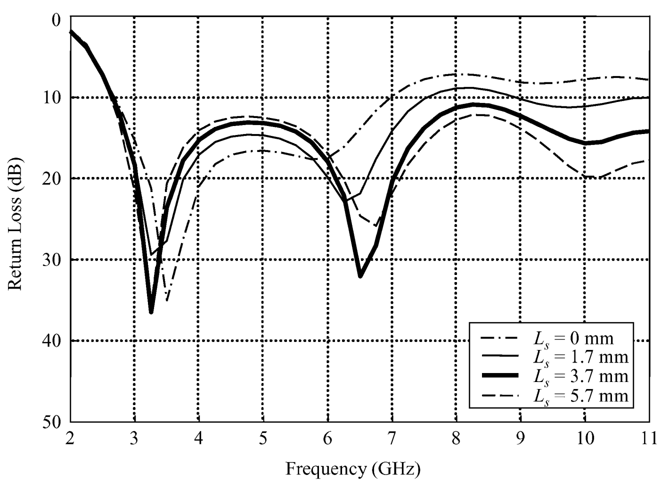

Fig. 5. Simulated return losses for the proposed antenna of various bevel length L_s with a fixed value of $W_s = 7$ mm. Other geometric parameters are the same as given in Fig. 2.

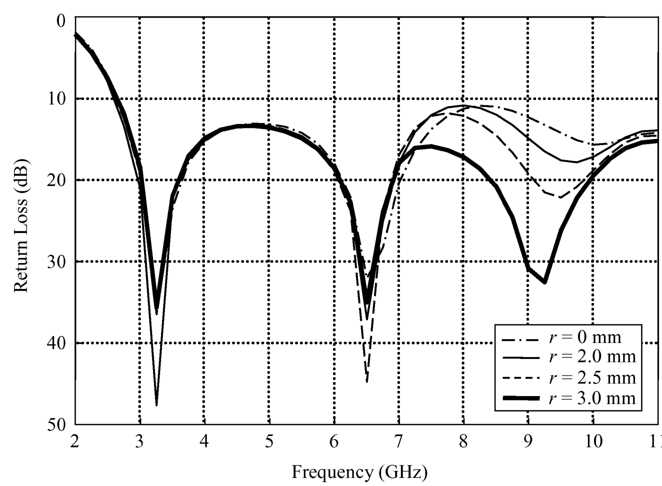

Fig. 7. Simulated return losses for the proposed antenna of various slot radii r with a fixed value of $W_e = 3$ mm. Other geometric parameters are the same as given in Fig. 1.

0 to 0.6 mm, the impedance matching at low frequencies can be greatly improved, at the expense of little deterioration in high frequency matching.

By comparing Figs. 1 to 3, it is found that L_a, L_g, and g are principally relevant to the low frequency characteristics, but not the high frequency performance. The reason is that in the low frequency band, the proposed antenna acts like as a printed monopole (or dipole) antenna, while in the high frequency band, the antenna behavior is like a slot antenna. Hence, properly designing the shape of the two bevels between the patch and ground plane will enhance the slot mode radiation and improve the impedance matching in high frequency band. Figs. 5 and 6 show the simulated return losses for various bevel sizes of the ground plane. It is clearly seen that changing W_s or L_s is an efficient way to improving the input impedance matching, especially at the high frequency. For the case of the bevel size $W_s = L_s = 0$ mm, which means no bevel on the ground plane, the bandwidth is not sufficient. Properly choose W_s and L_s, a widest bandwidth can be obtained. From the simulated results in Figs. 5 and 6, it occurs when $W_s = 7$ mm and $L_s = 3.7$ mm.

Additionally, two semicircle slots cut in the bottom side of the ground plane may further improve the antenna performance. The effects of different radii and positions of the semicircle slots were investigated. The simulated return losses for various sizes and positions of the semicircle slot are shown in Figs. 7 and 8. It can be seen in Fig. 7 that the return loss curves have similar shapes for the three different slot radii ($r = 2.0$, 2.5, and 3.0 mm) at low frequencies, but the high frequency impedance matching changes significantly with the variation of r. In Fig. 8, when W_e becomes larger (i.e., becoming farther from the side edge of the ground plane), the high frequency matching is slightly improved.

The radiation pattern in low frequency band is omnidirectional, but it usually deteriorates in the high frequency region. It is because that at the high frequencies, the magnetic currents mainly distributed over the slots between the radiation patch and the ground plane. The waves travel through the slots cause directional radiation patterns in the horizontal plane (i.e., the xz-plane). By introducing these two semicircle slots, the

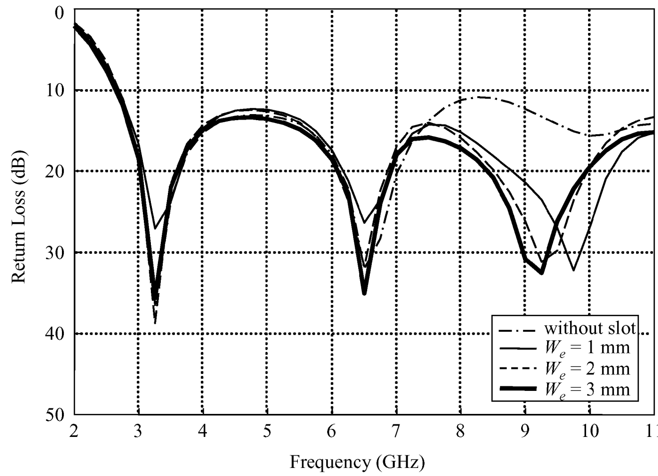

Fig. 8. Simulated return losses for the proposed antenna of various distance W_e with a fixed value of $r = 3$ mm. Other geometric parameters are the same as given in Fig. 1.

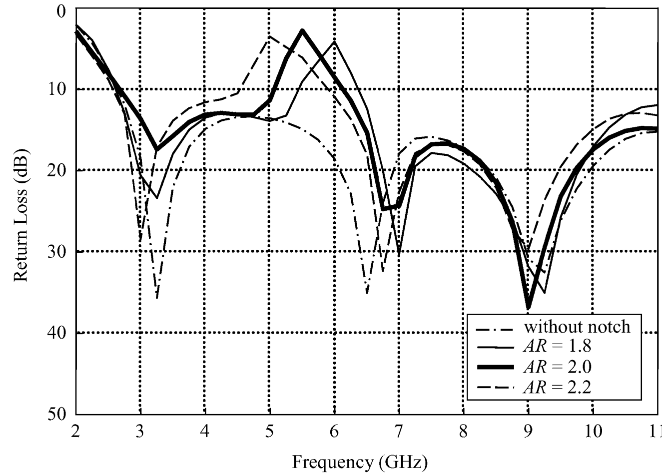

Fig. 10. Simulated return losses for the proposed antenna of various axial ratio (AR), the minor axis is 2.3 mm with a fixed value of $W_c = 3.6$ mm. Other geometric parameters are the same as given in Fig. 1.

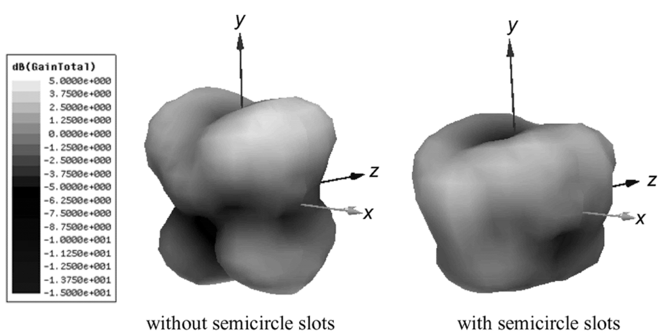

Fig. 9. Simulated 3-D radiation patterns with and without semicircle slots in the ground plane of the proposed antenna at 9 GHz.

transverse currents on the ground plane near the bottom side diminish. Thus the waves radiated from the slot propagate in a more omnidirectional way. Also, since the currents on the ground plane at high frequencies are rectified with the insertion of the two semicircle slots, more power is fed into the slots between the patch and the ground plane. As the results, the return-loss bandwidth of the antenna is broadened, and the gains in high frequency band become larger. Fig. 9 shows the comparison of the simulated 3-D radiation patterns with and without the semicircle slots at 9 GHz. In Fig. 9, the radiation pattern with semicircle slots is more omnidirectional than that without slots in the horizontal plane (i.e., the xz-plane).

B. UWB Antenna With Band-Notched Function Design

The frequency range for UWB systems approved by the FCC is between 3.1 to 10.6 GHz. It might cause interference to the existing wireless communication systems, for example the WLAN operating in 5.15–5.85 GHz. Therefore, the UWB antenna with a band-notched characteristic is required.

To obtain the band-notched function, the concept of the parallel LC circuit is applied. At resonant frequency, the parallel LC circuit will cause high input impedance that leads to the desired high attenuation and impedance mismatching near the notch frequency. In this paper, a pair of T-shaped stubs is embedded inside an elliptical slot cut in the radiation patch to form the parallel LC circuit. The elliptical slot and the T-shaped stubs are equivalent to an inductor and a capacitor, respectively. By adjusting the inductor and capacitor values, the suitable notch frequency and bandwidth can be achieved.

Fig. 10 shows the simulated return losses for various axial ratios (AR) of the elliptical slot with the minor axis fixed at 2.3 mm. It is seen that, increasing the axial ratio, which is similar to increasing the inductor value of the parallel LC circuit, has the effects of adjusting the center notch frequency as well as increasing the notch bandwidth. When AR varies from 1.8 to 2.2 mm, the center notch frequency varies from 6 to 5 GHz. On the other hand, as W_c increases, the rejection-band region moves toward lower frequency with a narrower notch bandwidth. It is similar to increasing the capacitor value of a parallel LC circuit. The simulated return losses for various W_c are shown in Fig. 11. When W_c varies from 2.6 to 5.6 mm, the center notch frequency varies from 6.5 to 4.75 GHz. Thus, the notch frequency can be adjusted by selecting the suitable W_c and AR.

In the case of $W_c = 3.6$ mm and $\mathrm{AR} = 2.2$, the resistance and reactance of the proposed antenna at 5.5 GHz are 112 Ω and 146 Ω, respectively. This high input impedance causes impedance mismatching at the notch frequency, and the band-notched function covering the WLAN frequencies is obtained. Based on the analysis described above, the optimized design value of each physical dimension of the proposed antenna is determined and as shown in Fig. 1. The simulated current distribution at 5.5 GHz is shown in Fig. 12. It reveals that the currents mainly concentrate over the area of the two T-shaped stubs inside the elliptical slot cut in the radiation patch.

IV. Experiment Results

The measured return losses of the proposed antenna with and without the band-notched function are also shown in Fig. 11. Without band-notched function, the antenna bandwidth (2:1 VSWR, or about 9.5 dB return loss) covers the range of 3.1–10.6 GHz assigned for the UWB application. Whereas with the band-notched function, the bandwidth is from 2.95 GHz to more than 11 GHz, and the antenna has a rejection

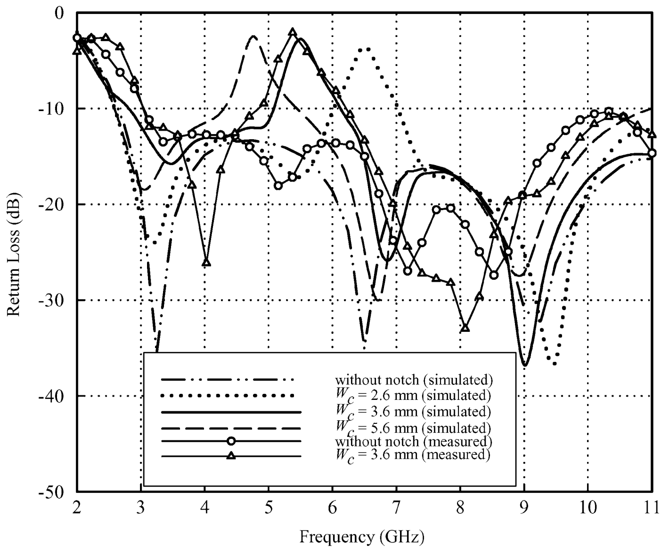

Fig. 11. Simulated and measured return losses of the proposed antenna for various T-shaped stub width W_c with a fixed value of $\mathrm{AR} = 2$. Other geometric parameters are the same as given in Fig. 1.

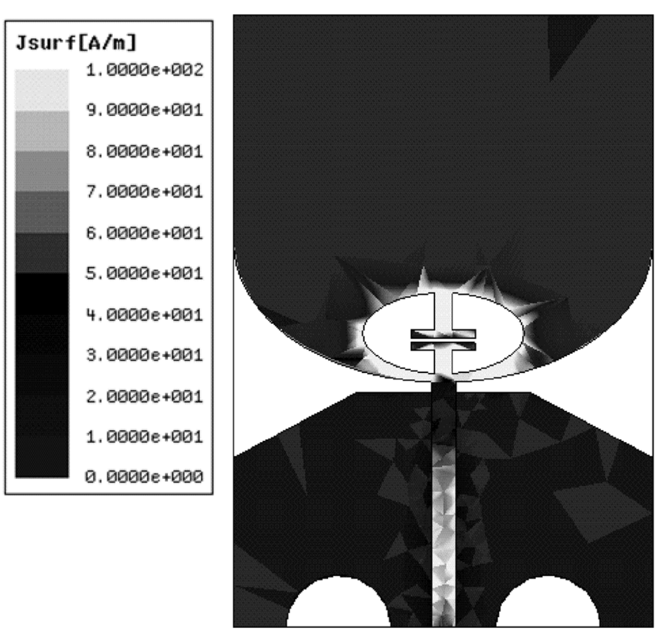

Fig. 12. Simulated current distribution of the proposed antenna at 5.5 GHz.

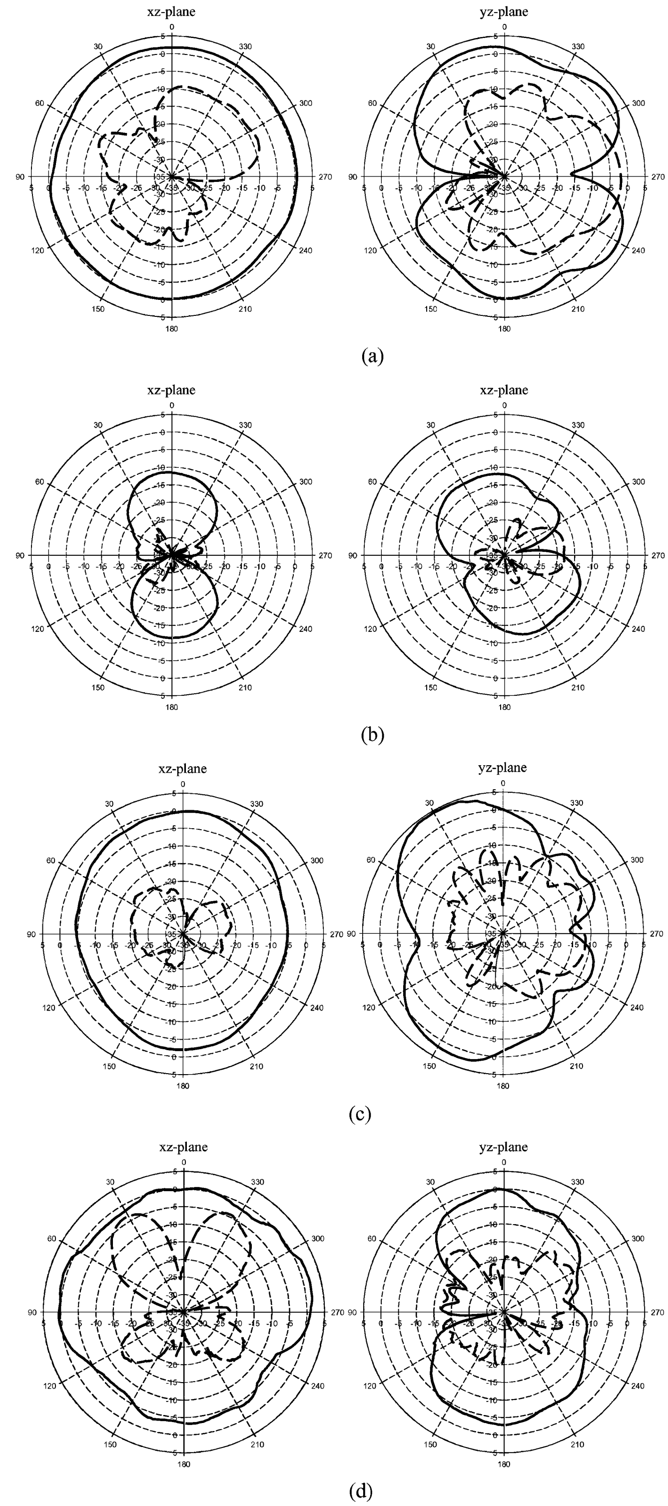

Fig. 13. Measured radiation patterns at (a) 3 GHz, (b) 5.5 GHz, (c) 6 GHz, and (d) 9 GHz. (solid line: E_ϕ dashed line: E_θ).

frequency band of 5 to 6 GHz, where the wireless LAN service is allocated, when inserting the equivalent parallel LC circuit into the radiation patch. An immediate sharp increase in VSWR is observed at the notch frequency.

Fig. 13 (a) to (d) shows the measured radiation patterns at 3, 5.5, 6, and 9 GHz, respectively. It can be seen that the patterns of the proposed antenna at frequencies out of the notched band present omnidirectional and stable radiation characteristics in the xz-plane (H-plane) over the operating frequency range, which are similar to that of the typical monopole antenna. The patterns measured at 5.5 GHz demonstrates that the antenna has much lower gains in the notched band than at other frequencies (3, 6, and 9 GHz), as shown in Fig. 13(b).

The measured antenna gains from 3 to 10 GHz of the realized antenna are shown in Fig. 14. The figure indicates that, the proposed antenna has good gain flatness except for in the notched band. The measured antenna gain variations are less than 4 dB throughout the desired UWB frequency band, and a sharp gain drop of about 10 dB occurs at 5.5 GHz.

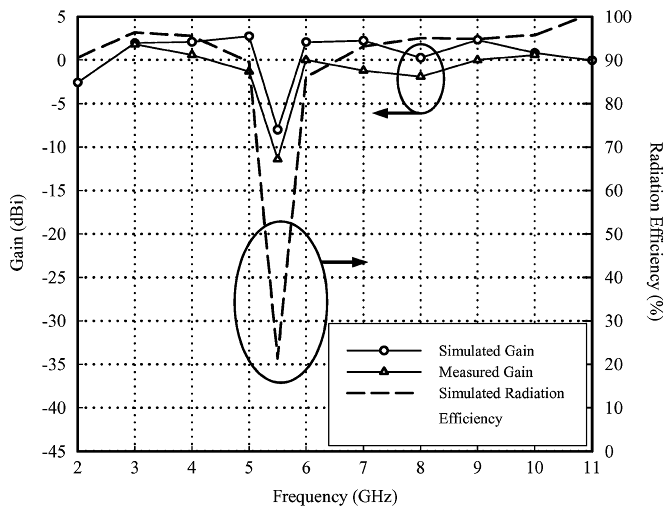

Fig. 14. Gains and radiation efficiency of the proposed antenna with band-notched function.

The reduction in gain at the notch frequency is significantly greater than the reduction of power fed into the antenna caused by the return loss. This phenomenon can be investigated by examining the radiation efficiency. In Fig. 14, the simulated radiation efficiency, which excludes the impedance mismatching effect, at 5.5 GHz is only about 21%. It is because that most currents are trapped in a small region of the equivalent parallel LC circuit at this frequency, as shown in Fig. 12, the resultant radiation fields cancel out, and thus the antenna does not radiate efficiently.

V. Conclusion

A compact microstrip-fed planar UWB antenna with the band-notched characteristic at around 5.5 GHz has been proposed and implemented. The total antenna size is 24 mm $\times$ 35 mm $\times$ 0.8 mm. Several design parameters have been investigated for the optimal design. By using two bevels on the upper side of the ground plane, the impedance matching in high frequency band can be improved. Moreover, adding two semicircle slots in the bottom side of the ground plane improve not only the input matching, but also the radiation characteristics at high frequencies. A pair of T-shaped stubs inside an elliptical slot, which is an equivalent parallel LC circuit, is realized to obtain the band-notched function. The center notch frequency and desired notch bandwidth are achieved by the properly designed equivalent capacitor and inductor values (i.e., W_c and AR of the elliptical slot). It is seen from the measured results that the proposed antenna has omnidirectional radiation patterns and a rather flat gain variation over the full UWB band expect for in the notched band. Therefore, the proposed antenna is suitable for the UWB communication applications and at the same time prevents interference with the WLAN systems.

References

[1] First Report and Order in the matter of Revision of Part 15 of the Commission's Rules Regarding Ultra-Wideband Transmission Systems, Released by Federal Communications Commission ET-Docket 98-153, Apr. 22, 2002.

[2] Batra *et al.*, "Multi-band OFDM physical layer proposal for IEEE 802.15 task group 3a," *IEEE Document 802.15-04-0493r1*, Sep. 2003.

[3] R. Kohno, M. McLaughlin, and M. Welborn, "DS-UWB physical layer submission to 802.15 task group 3a," *IEEE Document 802.15-04-0137r4*, Jan. 2005.

[4] J. Y. Sze and K. L. Wong, "Bandwidth enhancement of a microstrip-line-fed printed wide-slot antenna," *IEEE Trans. Antennas Propag.*, vol. 49, pp. 1020–1024, Jul. 2001.

[5] X. Qing, M. Y. W. Chia, and X. Wu, "Wide-slot antenna for UWB Applications," in *Proc. IEEE AP-S Int. Symp.*, Jun. 2003, vol. 1, pp. 834–837.

[6] R. Chair, A. A. Kishk, and K. F. Lee, "Ultrawide-band coplanar waveguide-fed rectangular slot antenna," *Antennas Wireless Propag. Lett.*, vol. 3, no. 1, pp. 227–229, 2004.

[7] S. H. Hsu and K. Chang, "Ultra-thin CPW-fed rectangular slot antenna for UWB applications," in *Proc. IEEE AP-S Int. Symp.*, Jul. 2006, pp. 2587–2590.

[8] H. D. Chen, "Broadband CPW-fed square slot antenna with a widened tuning stub," *IEEE Trans. Antennas Propag.*, vol. 51, pp. 1982–1986, Aug. 2003.

[9] Y. Liu, K. L. Lau, and C. H. Chan, "Microstrip-fed wide slot antenna with wide operating bandwidth," in *Proc. IEEE AP-S Int. Symp.*, Jun. 2004, vol. 3, pp. 2285–2288.

[10] Y. W. Jang, "A circular microstrip-fed single-layer single-slot antenna for multi-band mobile communications," *Microw. Opt. Technol. Lett.*, vol. 37, pp. 59–62, Apr. 2003.

[11] T. Yang and W. A. Davis, "Planar half-disk antenna structures for ultra-wideband communications," in *Proc. IEEE AP-S Int. Symp.*, Jun. 2004, vol. 3, pp. 2508–2511.

[12] N. P. Agrawall, G. Kumar, and K. P. Ray, "Wide-band planar monopole antennas," *IEEE Trans. Antennas Propag.*, vol. 46, no. 2, pp. 294–295, Feb. 1998.

[13] L. Jianxin, C. C. Chiau, X. Chen, and C. G. Parini, "Study of a printed circular disc monopole antenna for UWB systems," *IEEE Trans. Antennas Propag.*, vol. 53, no. 11, pp. 3500–3504, Nov. 2005.

[14] M. J. Ammann and Z.-N. Chen, "Wideband monopole antennas for multi-band wireless systems," *IEEE Antennas Propag. Mag.*, vol. 45, no. 2, pp. 146–150, Apr. 2003.

[15] J. N. Lee and J. K. Park, "Impedance characteristics of trapezoidal ultra-wideband antennas with a notch function," *Microw. Opt. Technol. Lett.*, vol. 46, no. 5, pp. 503–506, Sep. 2005.

[16] H. K. Lee, J. K. Park, and J. N. Lee, "Design of a planar half-circle-shaped UWB notch antenna," *Microw. Opt. Technol. Lett.*, vol. 47, no. 1, pp. 9–11, Oct. 2005.

[17] K. L. Wong, Y. W. Chi, C. M. Su, and F. S. Chang, "Band-notched ultra-wideband circular-disk monopole antenna with an arc-shaped slot," *Microw. Opt. Technol. Lett.*, vol. 45, no. 3, pp. 188–191, May 2005.

[18] C. Y. Huang, W. C. Hsia, and J. S. Kuo, "Planar ultra-wideband antenna with a band-notched characteristic," *Microw. Opt. Technol. Lett.*, vol. 48, no. 1, pp. 99–101, Jan. 2006.

[19] C. Y. Huang and W. C. Hsia, "Planar ultra-wideband antenna with a frequency notch characteristic," *Microw. Opt. Technol. Lett.*, vol. 49, no. 2, pp. 316–320, Feb. 2007.

[20] H. Yoon, H. Kim, K. Chang, Y. J. Yoon, and Y. H. Kim, "A study on the UWB antenna with band-rejection characteristic," in *Proc. IEEE AP-S Int. Symp.*, Jun. 2004, vol. 2, pp. 1784–1787.

[21] I. J. Yoon, H. Kim, K. Chang, Y. J. Yoon, and Y. H. Kim, "Ultra wide-band tapered slot antenna with band-stop characteristic," in *Proc. IEEE AP-S Int. Symp.*, Jun. 2004, vol. 2, pp. 1780–1783.

[22] S. Y. Suh, W. L. Stutzman, W. A. Davis, A. E. Waltho, K. W. Skeba, and J. L. Schiffer, "A UWB antenna with a stop-band notch in the 5-GHz WLAN band," in *Proc. IEEE ACES Int. Conf.*, Apr. 2005, pp. 203–207.

[23] Y. Gao, B. L. Ooi, and A. P. Popov, "Band-notched ultra-wideband ring-monopole antenna," *Microw. Opt. Technol. Lett.*, vol. 48, no. 1, pp. 125–126, Jan. 2006.

[24] K. H. Kim, Y. J. Cho, S. H. Hwang, and S. O. Park, "Band-notched UWB planar monopole antenna with two parasitic patches," *Electron. Lett.*, vol. 41, no. 14, pp. 783–785, Jul. 2005.

[25] W. J. Lui, C. H. Cheng, and H. B. Zhu, "Frequency notched printed slot antenna with parasitic open-circuit stub," *Electron. Lett.*, vol. 41, no. 20, pp. 1094–1095, Sep. 2005.

[26] HFSS. Pittsburgh, PA, Ansoft Corporation.

Chong-Yu Hong was born on June 16, 1982, in Taipei, Taiwan, R.O.C. He received the B.S. degree in electrical engineering from Tamkang University, Tamsui, Taiwan, R.O.C., in 2004, and M.S. degree in communication engineering from National Chiao Tung University, Hsinchu, Taiwan, R.O.C., in 2006.

He is currently with the Chi Mei Communication Systems Incorporation, Taipei, Taiwan, R.O.C.

Ching-Wei Ling was born on January 2, 1980, in Nantou, Taiwan, R.O.C. She received the B.S. and M.S. degrees in physics from the National Kaohsiung Normal University, Kaohsiung, Taiwan, in 2004. She is currently working toward the Ph.D. degree in communication engineering in the National Chiao Tung University, Hsinchu, Taiwan, R.O.C.

Her current research interests include UWB systems and microwave circuits.

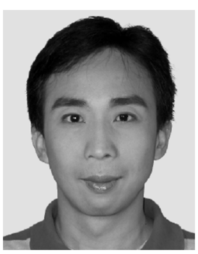

I-Young Tarn was born in Taipei, Taiwan, R.O.C. He received the B.S. and M.S. degrees in electrical engineering from Yuan-Ze University, Tao-Yuan, Taiwan, R.O.C., in 1993 and 1995, respectively, He is currently working toward the Ph.D. degree in communication engineering at the National Chiao Tung University, Hsinchu, Taiwan, R.O.C.

From 1995 to 1999, he was an Assistant Researcher on the Systems Engineering Project, National Space Program Office, Hsinchu, Taiwan, R.O.C. Since 2000, he has been with the Electrical Engineering Division of the National Space Program Office, where he has been involved in satellite communications and antenna design. His research interests include microwave/mm-wave planar antennas, reflectarray antennas, circular polarization selective structures and satellite antenna design and verification.

Shyh-Jong Chung (M'92–SM'06) was born in Taipei, Taiwan, R.O.C. He received the B.S.E.E. and Ph.D. degrees from the National Taiwan University, Taipei, Taiwan, R.O.C., in 1984 and 1988, respectively.

Since 1988, he has been with the Department of Communication Engineering, National Chiao Tung University, Hsinchu, Taiwan, R.O.C., where he is currently a Professor. From September 1995 to August 1996, he was a Visiting Scholar in the Department of Electrical Engineering, Texas, A&M University, College Station. He was the leader of a sub-program in the four-year "Advanced Technologies for Telecommunications" national research program, which was sponsored by the Ministry of Education, Taiwan, R.O.C. He has authored or coauthored over 70 technical papers in international journals of conferences, including several invited papers and speeches. His areas of interest include the designs and applications of active and passive planar antennas, communications in ITSs, low-temperature co-fired ceramic (LTCC)-based RF components and modules, packaging effects of microwave circuits, and numerical techniques in electromagnetic.